THE JOURNAL OF BIOLOGICAL CHEMISTRY
Vol. 274, No. 49, Issue of December 3, pp. 34974–34980, 1999

Printed in U.S.A.

Role of Reactive Oxygen Species and p53 in Chromium(VI)-induced Apoptosis*

(Received for publication, June 15, 1999, and in revised form, September 2, 1999)

Jianping Ye‡, Suwei Wang‡§, Stephen S. Leonard‡§, Yi Sun¶, Leon Butterworth‡, Jim Antonini‡, Min Ding‡, Yongyut Rojanasakul§, Val Vallyathan‡, Vincent Castranova‡, and Xianglin Shi‡‖

From the ‡Health Effects Laboratory Division, National Institute for Occupational Safety and Health, Morgantown, West Virginia 26505, the §Department of Basic Pharmaceutical Sciences, West Virginia University, Morgantown, West Virginia 26506, and the ¶Department of Molecular Biology, Parke-Davis Pharmaceutical Research, Division of Warner-Lambert, Ann Arbor, Michigan 48105

Apoptosis is a programmed cell death mechanism to control cell number in tissues and to eliminate individual cells that may lead to disease states. The present study investigates chromium(VI) (Cr(VI))-induced apoptosis and the role of reactive oxygen species (ROS) and p53 in this response. Treatment of human lung epithelial cells (A549) with Cr(VI) caused apoptosis as measured by DNA fragmentation, mitochondria damage, and cell morphology. Cr(VI)-induced apoptosis is contributed to ROS generation, resulting from cellular reduction of Cr(VI) as measured by flow cytometric analysis of the stained cells, oxygen consumption, and electron spin resonance spin trapping. Scavengers of ROS, such as catalase, aspirin, and *N*-acetyl-L-cysteine, decreased Cr(VI)-induced apoptosis, whereas NADPH and glutathione reductase, enhancers of Cr(VI)-induced ROS generation, increased it. p53 is activated by Cr(VI), mostly by ROS-mediated free radical reactions. Cr(VI)-induced ROS generation occurred within a few minutes after Cr(VI) treatment of the cells, whereas p53 induction took at least 5 h. The level of Cr(VI)-induced apoptosis was similar in both p53-positive cells and p53-negative cells independent of p53 status in the early stage (0–3 h) of Cr(VI) treatment. However, at the later stage (3–24 h), the level of the apoptosis is higher in p53-positive cells than in p53-negative cells. These results suggest that ROS generated through Cr(VI) reduction is responsible to the early stage of apoptosis, whereas p53 contributes to the late stage of apoptosis and is responsible for the enhancement of Cr(VI)-induced apoptosis at this stage.

Apoptosis is a process in which cell death is initiated and completed in an orderly manner through activation and/or synthesis of gene products necessary for cell destruction (1). It is a response to physiologic and pathologic stresses that disrupt the balance between the rates of cell division and elimination. In diseases such as cancer, there is an imbalance between the rate of cell proliferation and cell death. Agents that promote or suppress apoptosis can alter the rates of cell division and death, influencing the anomalous accumulation of neoplastic cells.

Although many questions remain to be answered, it is generally believed that in certain cell types, oxidative stress is a critical part of the apoptotic process (2). It has been reported that oxidant or oxidant-promoting agents cause necrosis at higher concentrations and apoptosis at lower concentrations (2). Antioxidants can inhibit or delay oxidative stress-induced apoptosis (2). Another important mediator of apoptosis is p53 (3, 4). Activation of p53 involves growth arrest and/or apoptosis. Recent studies indicate that reactive oxygen species (ROS)[1] are downstream mediators of p53-dependent apoptosis (4, 5). p53 results in apoptosis through a multi-step process (4): (*a*) the transcriptional induction of redox-related genes; (*b*) the generation of ROS; and (*c*) the oxidative degradation of mitochondrial components, leading to apoptosis.

The present study focuses on Cr(VI)-induced apoptosis. Cr(VI) compounds are highly toxic and carcinogenic (6). They are potent inducers of tumors in experimental animals. They cause DNA damage, such as DNA strand breaks and dG hydroxylation (6). Earlier studies have shown that in cellular systems, Cr(VI) is reduced by certain flavoenzymes such as glutathione reductase to generate Cr(V) (7–9). During this process, molecular oxygen is reduced to O_2^-, which generates H_2O_2 via dismutation (7). The resultant Cr(V) reacts with H_2O_2 to generate $^{\cdot}OH$ radical via a Fenton-like reaction. Thus, during the one-electron reduction of Cr(VI), a whole spectrum of ROS are generated. Through ROS-mediated reactions, Cr(VI) is able to cause DNA damage (10) and activation of nuclear transcription factor NF-κB (11).

It is generally believed that ROS play an important role in carcinogenesis induced by a variety of carcinogens. The net effect of the response is determined by a balance between intercellular oxidants and antioxidants. ROS-mediated reactions are believed to play a key role in Cr(VI)-induced DNA damage. Cell cycle surveillance mechanisms set checkpoints for cell cycle progression. If the cell is damaged by external agent, such as Cr(VI), that may cause DNA breaks, cell cycle progression will be transiently delayed to allow the cell to repair the damaged DNA. If the DNA is severely damaged, the cell will undergo apoptosis (12). Apoptosis is a defense mechanism by which the body can eliminate damaged cells. Thus investigation on the role of ROS in Cr(VI) induced apoptosis is important to understand the mechanism of carcinogenesis caused by not only Cr(VI) but also by other carcinogens. We report here that Cr(VI) is a direct ROS promoting agent that causes mitochon-

* The costs of publication of this article were defrayed in part by the payment of page charges. This article must therefore be hereby marked "*advertisement*" in accordance with 18 U.S.C. Section 1734 solely to indicate this fact.

‖ To whom correspondence should be addressed: Pathology and Physiology Research Branch, National Inst. for Occupational Safety and Health, 1095 Willowdale Rd., Morgantown, WV 26505. Tel.: 304-285-6158; Fax: 304-285-5938; E-mail: xas0@cdc.gov.

[1] The abbreviations used are: ROS, reactive oxygen species; Cr(VI), potassium dichromate; Cr(III), chromium fluoride; ESR, electron spin resonance; NAPDH, β-nicotinamide adenine dinucleotide phosphate; NAC, *N*-acetyl-L-cysteine; DCFH-DA, 2′,7′-dichlorofluorescin diacetate; CsA, cyclosporine A; SOD, superoxide dismutase; PBS, phosphate-buffered saline; FACS, fluorescence-activated cytometry sorter; DMPO, 5,5-dimethyl-1-pyrroline *N*-oxide.

dria damage and induces apoptosis. The apoptotic processes involves both p53-independent and p53-dependent pathways.

MATERIALS AND METHODS

Reagents—Potassium dichromate (Cr(VI)) and chromium fluoride (Cr(III)) were purchased from Aldrich. Chromium-GSH complex (Cr(IV)) was synthesized according to the method described earlier (13). Aspirin, β-nicotinamide adenine dinucleotide phosphate (NADPH), *N*-acetyl-L-cysteine (NAC), DCFH-DA, and cyclosporine A (CsA) were purchased from Sigma. Superoxide dismutase (SOD) and catalase were purchased from Roche Molecular Biochemicals. Dihydroethidium, JC-1, and $DiOC_6$ were purchased from Molecular Probe (Eugene, OR).

Cell Culture—The human lung epithelial cell lines (A549 and H1299) and the human prostate epithelial cell line PC3 were purchased from the American Type Culture Collection (Manassas, VA). The cells were cultured at 37 °C in a 5% CO_2 incubator with RPMI 1640 cell culture medium that was supplemented with 5% fetal calf serum, 2 mM L-glutamine, 100 units/ml penicillin, and 100 μg/ml streptomycin. The cells form a monolayer at confluence. Trypsin (0.25%) EDTA solution was used to detach the cells from the culture flask for plating and passing the cells.

Apotosis Assay—The cells were plated in a 96-well plate at a density of 2×10^4 cells/well in supplemented RPMI 1640 and incubated for16 h before the cells were subjected to treatment in triplicate wells. After treatment, the cells were washed twice in phosphate-buffered saline (PBS) (2.68 mM KCl, 1.47 M KH_2PO_4, 8 mM Na_2KPO_4, 136.75 mM NaCl), and apoptosis was quantitated by measuring the levels of cytosolic histone-bound DNA fragments. This was done by using a cell death enzyme-linked immunosorbent assay kit manufactured by Roche Molecular Biochemicals. The assays were carried out according to the protocol provided by the manufacturer. Briefly, the cells were lysed with 200 μl of lysis buffer at room temperature. The lysate from three identical wells was combined, and 20 μl of the resulted lysate was mixed with 80 μl of antibody solution in a well of the enzyme-linked immunosorbent assay plate. The loaded wells were incubated at room temperature for 2 h. The substrate was added after the wells were washed three times in washing buffer. After incubation at 37 °C for 10–20 min, the reaction was stopped, and optical density was measured using a microplate reader at a wavelength of 405 nm. The readings were used to represent the degree of apoptosis. A mean value of three separate experiments was for analysis.

Morphological Analysis—Apoptosis was also examined by morphological analysis. At the end of chromium treatment, the cells were washed twice in PBS and then fixed with 10% buffered formalin. The cells were stained with Wright staining kit containing solutions A, B, and C (Volu-Sol, Inc., Louisville, KY). The staining was conducted in a 96-well tissue culture plate according to the manufacturer's protocol. The cells were stained in 100 μl of Wright's stain solution (solution A) for 2 min, treated with 100 μl solution B for 1.5 min, and then rinsed in solution C for 10 s. After being air-dried, the stained cells were observed under a Leitz inverted microscope. The cell image was captured with a Sony 3CCD color video camera and printed with a Sony color video printer.

Fluorescence-activated Cytometry Sorter Analysis—The sample cells were suspended in 1 ml of PBS containing 0.1 mg/ml propidium iodine 5 min before flow cytometry assay. JC-1 was excited at 490 nm and detected at 600 nm. $DiOC_6$ was excited at 488 nm and detected at 525 nm. Dihydroethidium was excited at 490 nm and detected at 620 nm. DCFH-DA was excited at 488 nm and detected at 525 nm.

Mitochondrial trans-Membrane Potential ($\Delta\psi_m$) Assay—JC-1 (14, 15) and $DiOC_6$ (16–18) are two mitochondria specific flourescent dye. They have been widely used in monitoring $\Delta\psi_m$. The dye was dissolved in Me_2SO and diluted with PBS at 1:1000. The cells were plated in a 6-well plate at 5×10^5/well 16 h before treatment. After the cells were treated with chromium, the diluted dyes were applied to the cells for 15 min at 37 °C. The final concentrations were 10 μg/ml for JC-1 and 40 nM for $DiOC_6$. Then the cells were washed twice in PBS and harvested for FACS analysis.

Cellular Superoxide (O_2^-) and H_2O_2 Assay—Dihydroethidium is a O_2^--specific dye (19, 20). Dihydroethidium was dissolved in Me_2SO at 2 mM and kept at −20 °C. The cells were plated in a 6-well plate at 5×10^5/well 16 h before treatment. Dihydroethidium was added into the cell culture 15 min before the treatment was completed, and the staining was carried out at 37 °C. The final Me_2SO concentration in the cells culture was 0.1%. Then the cells were washed in PBS and harvested for FACS analysis. In the case of cellular image, the cells (2×10^4/well) were plated onto a glass slip in the 24-well plate. After being stained, the cells were washed in PBS and fixed with 10% buffered formalin. The slip was mounted on a glass slide and observed using a Saratro 2000 (Molecular Dynamics, Inc., Sunnyrale, CA) laser scanning confocal microscope (Optiphot-2, Nikon, Inc., Melville, PA) fitted with an argon-ion laser. DCFH-DA has been used frequently to monitor oxidative burst (5) and H_2O_2 level inside the cells (17, 21). Under the same condition, DCFH-DA (5 μM) was used to stain H_2O_2 inside the cells.

p53 Protein Assay—p53 protein was analyzed by Western blot assay. The cells were plated in a 100-mm culture dish and treated with chromium. The nuclear protein was prepared as described before (22). Briefly, 5×10^7 cells were treated with 500 μl of lysis buffer (50 mM KCl, 0.5% Nonidet P-40, 25 mM HEPES, pH 7.8, 1 mM phenylmethylsulfonyl fluoride, 10 μg/ml leupeptin, 20 μg/ml aprotinin, 100 μM dithiothreitol) on ice for 4 min. After 1 min of centrifugation at 14,000 rpm, the supernatant was saved as a cytoplasmic extract. The nuclei were washed once with the same volume of buffer without Nonidet P-40 and then were treated with 300 μl of extraction buffer (500 mM KCl, 10% glycerol with the same concentrations of HEPES, phenylmethylsulfonyl fluoride, leupeptin, aprotinin, and dithiothreitol as the lysis buffer) and pipetted several times. After centrifugation at 14,000 rpm for 5 min, the supernatant was harvested as the nuclear protein extract and stored at −70 °C. The protein concentration was determined using BCA protein assay reagent (Pierce). A standard Western blot was carried out to detect p53 protein level in 10 μg of the nuclear protein. Monoclonal p53 antibody (sc-126) was purchased from Santa Cruz Biotechnology (Santa Cruz, CA).

Oxygen Consumption Measurements—Oxygen consumption measurements were carried out using Gilson oxygraph equipped with a Clark electrode (Gilson Medical Electronics, Middledton, WI). Measurements were made from mixtures containing 1.0×10^6/ml cells, 300 μM Cr(VI), 300 μM Cr(IV), 300 μM Cr(III), and 1 mM NADPH in a total volume of 1.5 ml. The oxygraph was calibrated with medium equilibrated with oxygen of known concentrations.

ESR Measurements—ESR spin trapping technique was used to detect short-lived free radical intermediates. This technique involves the addition-type reaction of a short-lived radical with a paramagnetic compound (spin trap) to form a relatively long-lived free radical product (spin adduct), which can then be studied using conventional ESR. The intensity of the signal is used to measure the amount of short-lived radicals trapped, and the hyperfine couplings of the spin adduct are generally characteristics of the original trapped radicals. The spin trapping is a method of choice for detection and identification of free radical generation because of its specificity and sensitivity. All ESR measurement were conducted using a Varian E9 ESR spectrometer and a flat cell assembly. Reactants were mixed in a test tube in a final volume of 500 μl. The reaction mixture was then transferred to a flat cell for ESR measurement. Hyperfine couplings were measured (to 0.1 G) and 1,1-diphenyl-2-picrylhydrazyl was used as a reference. The relative radical concentration was estimated by multiplying half of the peak height by $(\Delta H_{pp})^2$, where ΔH_{pp} represents peak-to-peak width. The program EPRDAP, version 2.0, was used for data acquisition and analysis.

RESULTS

Induction of Apoptosis by Cr(VI)—The human lung tumor cell line, A549, was used to study Cr(VI)-induced apoptosis. DNA fragmentation assay was carried out by detection of histone-bound DNA fragments in a whole cell lysate with a cell death enzyme-linked immunosorbent assay system as stated under "Materials and Methods." Indeed, Cr(VI) was able to induce apoptosis in A549 cells. The induction of apoptosis is dose-dependent (Fig. 1*A*). The apoptosis increased with Cr(VI) concentrations from 75 to 300 μM, saturated at a dose above 300 μM, and decreased slightly at 500 μM. Thus, 300 μM was used for all experiments in this study. At this concentration, Cr(VI)-induced apoptosis depended upon incubation time (Fig. 1*B*). The earliest time for DNA fragmentation to be detectable was 2 h after the Cr(VI) treatment. The DNA fragmentation increased thereafter until 24 h and then decreased (Fig. 1*B*)

Observation of the cell morphology also indicates that Cr(VI) is able to induce apoptosis in the lung type II epithelial cells (Fig. 2). The Cr(VI)-treated cells undergo condensation of both the cytoplasm and the nucleus, which is typical of the apoptotic process.

Mitochondria are the limiting factor in the apoptosis pathway in many experimental systems (23). Disruption of mitochondria transmembrane potential ($\Delta\psi_m$) has been an established indicator of mitochondrial damage in the progression of apoptosis (14, 19). Two mitochondria-specific dyes, JC-1 (13, 14) and $DiOC_6$ (16–18), were employed for this purpose, and FACS analysis was conducted. The result shows that at 16 h post-treatment with 300 μM Cr(VI), $\Delta\psi_m$ was significantly reduced (Fig. 3). The gated population of stained cells dropped from 98 to 63% for JC-1 staining and from 82 to 67% for $DiOC_6$ staining, confirming damage at the mitochondrial level, which may be related to the apoptotic response of the cells to Cr(VI).

Role of p53 in the Metal-induced Apoptosis—The tumor suppressor gene product, p53, has been reported to mediate apoptosis in many experimental systems. It is believed that this activity is responsible for the tumor suppressive function of p53 (24–26). This section examines whether p53 protein is involved in Cr(VI)-induced apoptosis. The p53 activity was studied by extracting nuclear protein from Cr(VI)-treated cells and monitoring the p53 protein by immunoblot analysis (Fig. 4). The p53 protein was detectable in the nuclear extract of the untreated cells (Fig. 4, *lane 1*). After an exposure to Cr(VI), the p53 protein level was elevated in a time-dependent manner. A Cr(VI)-induced increase in p53 was not noticeable at 0.5, 1, 2, or 3 h during the period of Cr(VI) treatment (Fig. 4, *lanes 2–5*). However, an increase in the p53 level was observed at 2 h after a 3-h incubation of the cells with Cr(VI) (Fig. 4, *lane 6*), and this increase reached its peak at 20 h after the treatment (Fig. 4, *lane 8*). Housekeeping transcription factor YY1 was used as a protein loading control.

The above results demonstrate that p53 was activated by Cr(VI) because nuclear p53 level was induced. The question to be answered is whether p53 activation contributed to the progression of Cr(VI)-induced apoptosis. p53-positive and -negative cell lines were employed to address this question. A549 is a p53-positive cell line. Both H1299, a human lung tumor cell line (25), and PC3, a human prostate tumor cell line (27), are p53-negative cells. These three cells types were treated for 3 h with Cr(VI) at different concentrations and examined for apoptosis 24 h later. The results show that, at all three concentrations, the p53-positive cells expressed much stronger apoptosis than the p53-negative cells (Fig. 5*A*). In the time course analysis, both A549 (p53+) and H1299 (p53−) cells were treated with 300 μM Cr(VI), and apoptosis was monitored at different times post-treatment (Fig. 5*B*). The results show that, at the early stage (<3 h), there was no difference between the p53-positive and -negative cells, indicating that p53 does not play a significant role at this stage of Cr(VI)-induced apoptosis. A difference in the rate of apoptosis was observed at 12 h post-treatment, and at 24 h, apoptosis in A549 cells was twice that found in H1299 cells. This difference in Cr(VI)-induced apoptosis exhibited in the p53 wild type and mutant type cells suggests that both p53-independent and p53-dependent pathways may be involved in at the later stage of Cr(VI)-induced apoptosis.

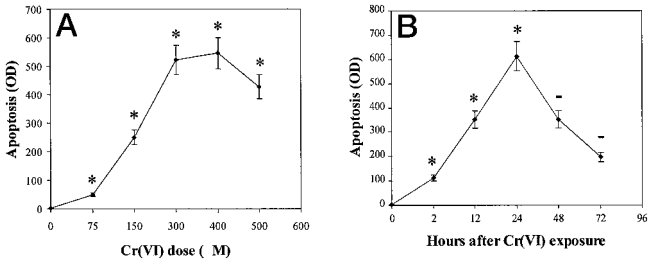

FIG. 1. **Cr(VI)-induced apoptosis.** *A*, A549 cells were seeded in a 96-well plate at a density of 1×10^4/well. Cr(VI) was added to the cell culture at the final concentrations indicated. After an exposure of 3 h, Cr(VI) was removed, and the culture was supplemented with the fresh cell medium. Histone protein assay was carried out 24 h later. *B*, the cells were treated with Cr(VI) at a final concentration of 300 μM for 3 h and then cultured in fresh cell medium. The histone protein assay was conducted at different times as shown after Cr(VI) treatment. The mean value ± S.D. were from the results of three independent experiments. * indicates a significant increase from control ($p < 0.05$). − indicates a significant decrease from the 24 h values ($p < 0.05$).

Detection of ROS Formation—ROS are considered to play a major role in Cr(VI)-induced carcinogenesis. For example, through ROS, Cr(VI) causes DNA damage (10, 28) and NF-κB activation (11, 29). We therefore examined ROS generation in the Cr(VI)-treated cells. The ability of Cr(VI) to generate $^{\cdot}OH$ radicals was examined using an ESR spin trapping method. Fig. 6*A* shows a typical ESR spectrum generated by cellular reduction of Cr(VI) from a reaction mixture containing Cr(VI) and A549 cells in pH 7.4 phosphate-buffered solution. The spectrum consists of an 1:2:2:1 quartet with splittings of $a_H = a_N = 14.9$ G, where a_N and a_H denote hyperfine splittings of the nitroxyl nitrogen and α-hydrogen, respectively. Based on these splittings and the 1:2:2:1 line shape (9), this spectrum was assigned to the DMPO/$^{-}$OH adduct, which is evidence of ^{-}OH radical generation. In the presence of NADPH, the signal was enhanced (Fig. 6*B*). The peak at $g = 1.9792$ was assigned to Cr(V) according to the value reported in the literature for the Cr(V) species (9). Addition of catalase completely eliminated the signals of DMPO/$^{\cdot}$OH (Fig. 6*C*), indicating that $^{\cdot}OH$ radical generation involves H_2O_2 via a Fenton-like reaction.

The ability of Cr(VI) to generate $O_2^{\cdot-}$, and H_2O_2 in the human epthelial cells was analyzed by intracellular staining of $O_2^{\cdot-}$ and H_2O_2. Hydroethidine, a specific fluorescent dye for $O_2^{\cdot-}$, and DCFH-DA, a fluorescent dye for H_2O_2, were applied to cells for tracking generation of ROS. The cells were examined with a laser scanning confocal microscope. Both $O_2^{\cdot-}$ and H_2O_2 were visualized inside the untreated cells (Fig. 7*A*, *Untreated*). Because these oxygen species are mainly produced in the mitochondria, the bright color fluorescent dots in the cytoplasm represent subcellular location of $O_2^{\cdot-}$ and H_2O_2, respectively. In

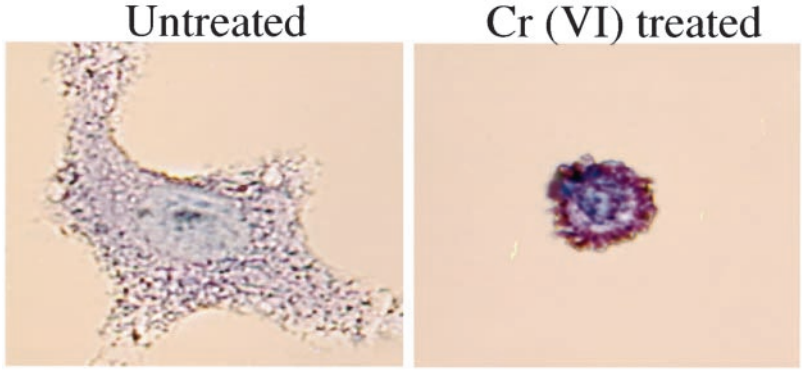

FIG. 2. **At 24 h after Cr(VI) treatment, the cell morphology was examined under a microscope at a magnification of 10 × 40, and the image was captured with an attached camcorder.**

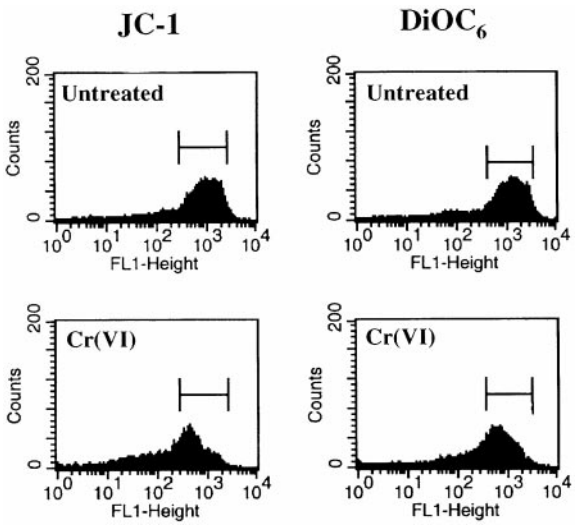

FIG. 3. **Mitochondrial damage and morphological assay.** The cells were treated with 300 μM Cr(VI) for 3 h, and mitochondrial trans-membrane potential was examined 16 h later by FACS with JC-1 or $DiOC_6$ staining.

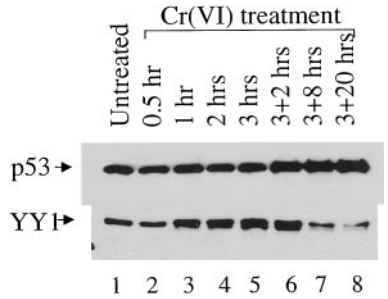

FIG. 4. **Cr(VI)-induced p53 activation.** p53 protein level was examined in 10 μg of the nuclear extract of A549 cells by Western blot after 300 μM Cr(VI) treatment. Monoclonal p53 antibody (sc-126, Santa Cruz Biotechnology) was used in the assay. *Lane 1*, untreated cells; *lanes 2–5*, p53 protein level examined immediately after 1, 2, or 3 h of 300 μM Cr(VI) treatment; *lanes 6–8*, p53 protein level examined 2, 8, or 24 h after 3 h of Cr(VI) treatment. YY1 serves as a protein loading control.

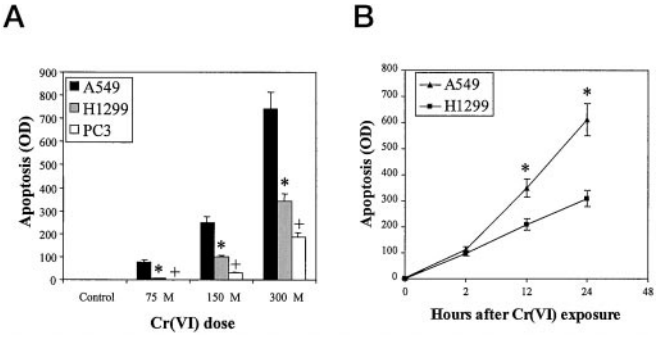

FIG. 5. **Role of p53 in Cr(VI)-induced apoptosis.** *A*, p53-positive (A549) and -negative (H1299, PC3) cell lines were treated with Cr(VI) at different concentrations as indicated. The histone protein assay was conducted of 24 h. * and + indicate a significant difference from A549 cells ($p < 0.05$). *B*, A549 and H1299 cells were treated with 300 μM Cr(VI), and histone protein assay was conduced at different times as indicated. * indicates a significant increase from H1299 cells ($p < 0.05$).

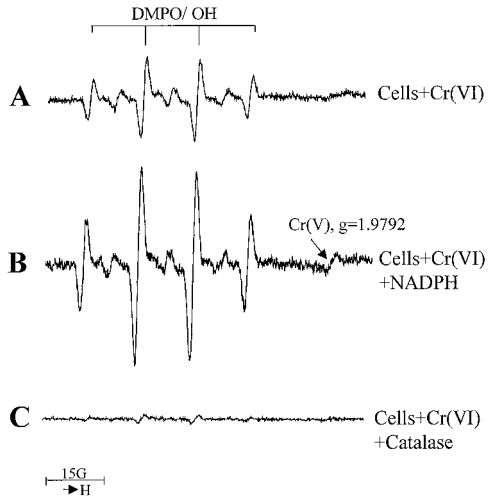

FIG. 6. **Measurement of Cr(VI)-induced ROS generation.** *A*, ESR spectrum was recorded 2 min after reaction initiation from a mixture containing1 $\times$ 10^6 A549 cells/ml, 1 mM Cr(VI) and 100 mM DMPO. *B*, same as *A* but with 1 mM NADPH added. *C*, same as *A* but with 5,000 units/ml catalase added.

the presence of Cr(VI), both O_2^- and H_2O_2 were dramatically enhanced (Fig. 7*A*, *Cr(VI) Treated*). This increase occurred within 30 min. Hydroethidine exhibits a red or orange color after being oxidized by O_2^-. DCFH-DA exhibits green and orange colors after being oxidized.

The generation of O_2^- and H_2O_2 was quantified by flow cytometry analysis of the stained cells. For O_2^-, the gated cell population increased from 36 to 62% after Cr(VI) treatment (Fig. 7*B*). In the presence of SOD, the Cr(VI)-induced population dropped from 62 to 46%. SOD treatment reduced the basal population from 36 to 30%. These results confirm at the cellular level that Cr(VI) induced ROS production after penetrating into the cells. In addition, SOD is able to pass the cell membrane and prevent accumulation of O_2^- resulting from reduction of Cr(VI). A similar result was obtained for H_2O_2 by flow cytometry (data not shown). Because O_2^- is the one-electron reduction product of molecular oxygen, the O_2 consumption from cells treated with Cr(VI) was measured using an oxygraph. As shown in Fig. 7*C*, Cr(VI) enhanced the O_2 consumption, and NADPH was able to accelerate it slightly. Cr(III) or Cr(IV) did not exhibit any observable activity.

Role of ROS in Cr(VI)-induced Apoptosis—Several strategies were used to investigate the role of the radicals in Cr(VI)-induced apoptosis. Different oxidative states of chromium were examined for their activity in induction of apoptosis. Cr(III), Cr(IV), and Cr(VI) exhibit different activities in the generation of free radicals, with Cr(VI) being the strongest one. Results of the apoptosis assay indicate that although Cr(III) and Cr(IV) were able to induce apoptosis slightly, their activities were much weaker than that of Cr(VI) (Fig. 8*A*). This is in line with the fact that Cr(VI) can be rapidly reduced to the lower oxidative state such as Cr(V) and ROS are generated during the reaction. In the presence of NADPH, the free radical production was enhanced (Fig. 6*B*). As reported earlier, glutathione reductase is another major Cr(VI) reductant. Both of these reagents promoted Cr(VI)-induced apoptosis (Fig. 8*B*). The effects of antioxidants were also examined in this experimental system. Catalase, (5), aspirin (30), and NAC (5) are established antioxidants. Their ability to block Cr(VI)-induced apoptosis were examined. The cells were pretreated with each of the three antioxidants and then analyzed for Cr(VI)-induced apoptosis. The results shows that all of three antioxidants were effective in inhibiting Cr(VI)-induced apoptosis (Fig. 8*C*). The reduction was 40% by catalase, 50% by aspirin, and 90% by NAC, demonstrating a role of ROS in the Cr(VI)-induced apoptosis.

The previous sections have shown that Cr(VI) is able to activate p53 and that p53 induction is involved in Cr(VI)-induced apoptosis. p53 is a transcription factor involved in the

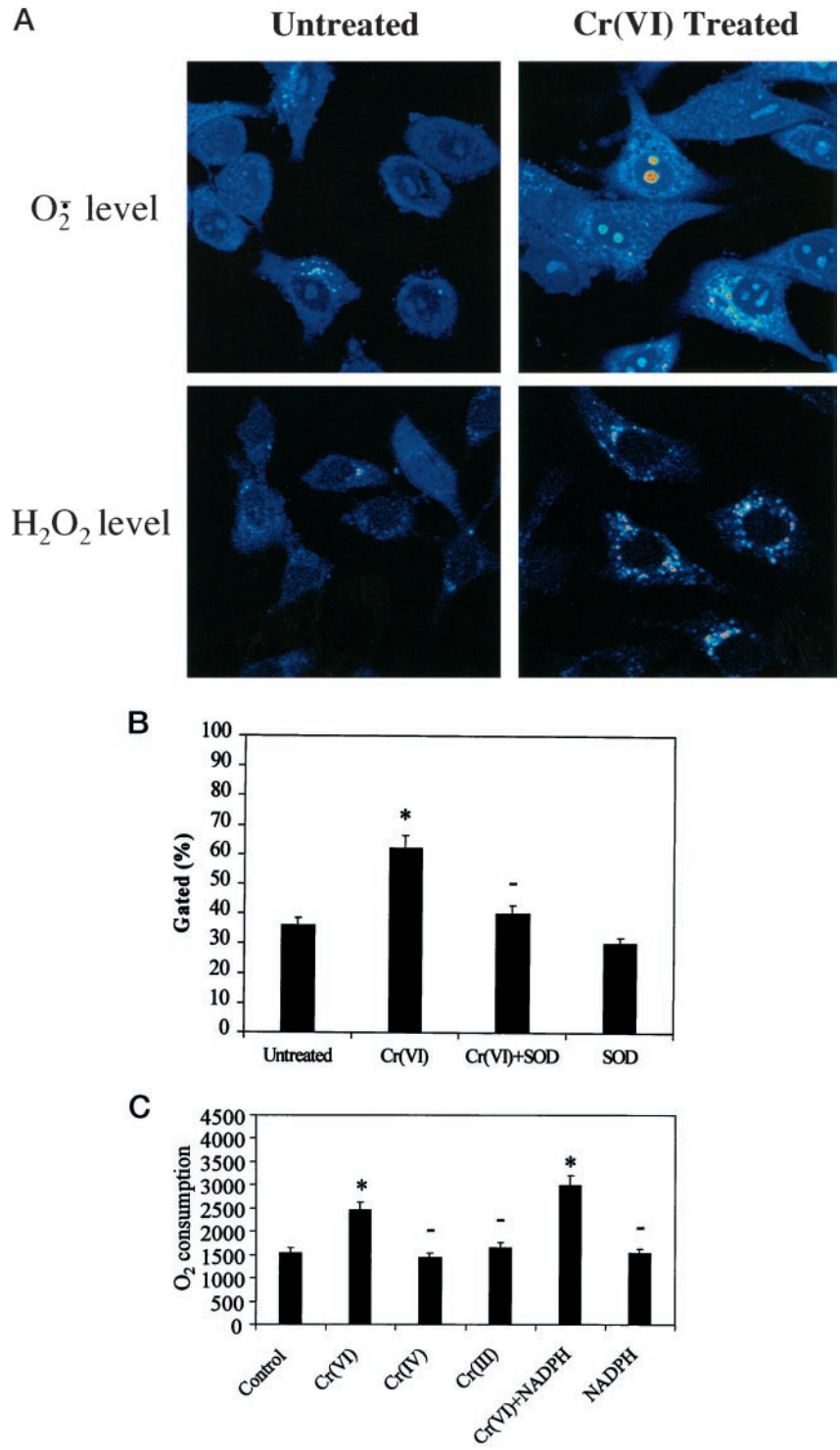

FIG. 7. **$O_2^{\cdot-}$ and H_2O_2 generation inside the cells and O_2 consumption.** *A*, for staining of $O_2^{\cdot-}$ and H_2O_2, A549 cells were treated with 300 μM Cr(VI) in the presence of 2 μM dihydroethidium or 5 μM DCFH-DA for 30 min. For $O_2^{\cdot-}$ and H_2O_2 image, the cells were washed once in PBS and fixed with 10% buffered formalin. The bright color dots in the cells represent $O_2^{\cdot-}$ and H_2O_2. The images were captured with a confocal microscope. *B*, quantitation of $O_2^{\cdot-}$ by FACS. SOD was used to pretreat the cells and inhibit accumulation of $O_2^{\cdot-}$ inside the cells. *C*, oxygen consumption by A549 cells treated with various agents as indicated. * indicates a significant increase from control ($p < 0.05$). − indicates no significant difference from control.

activation of man oxidative stress genes (4). It has been reported that p53 gene product causes apoptosis using ROS as downstream mediators. Because there are two mechanisms of ROS generation, the direct generation of ROS from Cr(VI) reaction and the p53-mediated transcriptional activation, this section examines which mechanism is critical for the initiation of apoptosis, focusing on the early events of apoptosis before p53 activation. Mitochondrial damage was observed in the early stage of Cr(VI) treatment. The damage was detected with FACS analysis of the JC-1-stained cells. In the presence of Cr(VI), the gated cell population was dropped from 36 to 25% within 2.5 h (Fig. 9*A*). CsA is an inhibitor of mitochondrial permeability transition (17). Inhibition of permeability transition leads to prevention of $\Delta\psi_m$ disruption. CsA was utilized to prevent the metal-induced mitochondrial damage. The result showed that CsA pretreatment can prevent Cr(VI)-induced $\Delta\psi_m$ disruption (Fig. 9*A*). CaA pretreatment also reduced Cr(VI)-induced DNA fragment (Fig. 9*B*), suggesting mitochondrial involvement in the initiation of Cr(VI)-induced apoptosis, which seems p53-independent.

DISCUSSION

The present study shows that Cr(VI) is able to cause apoptosis in the epithelial cell line A549. ROS are involved in the apoptotic response. The following experimental observations support this conclusion: (*a*) Reaction of Cr(VI) with cells gen-

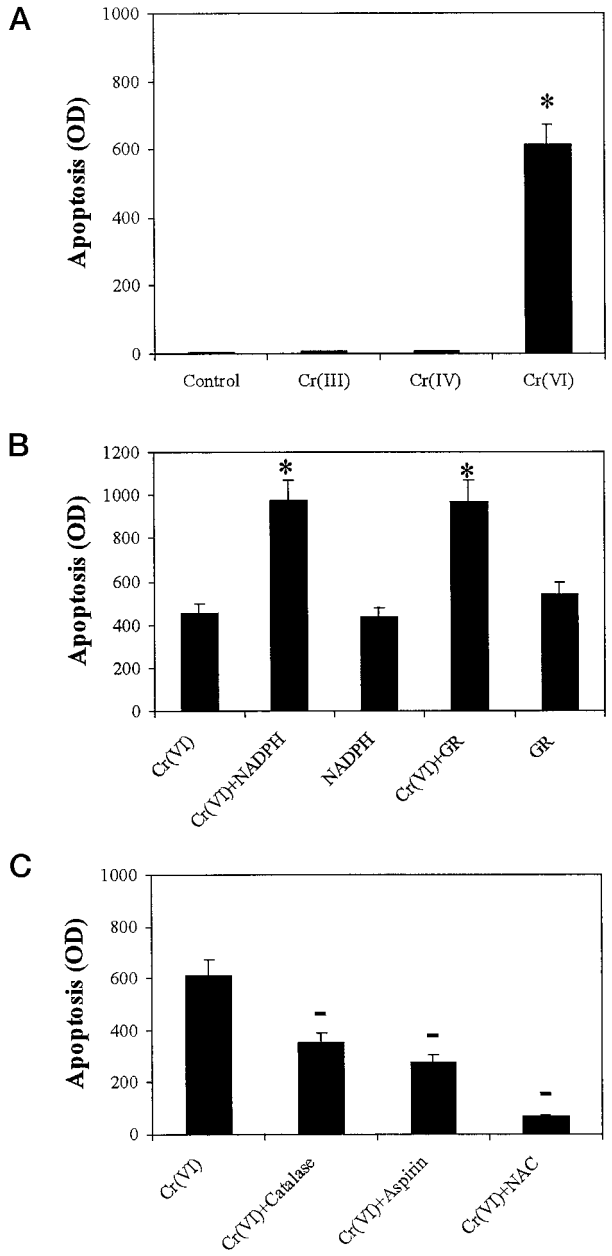

FIG. 8. **Role of ROS in Cr(VI)-induced apoptosis.** *A*, the cells were treated with Cr(VI), Cr(IV), or Cr(III) at a final concentration of 300 μM for 3 h. The histone protein assay was conduced 24 h later. *B*, the cells were treated with 300 μM Cr(VI) in the presence NADPH or glutathione reductase for 3 h. The histone protein assay were carried out 24 h later. *C*, the cells were pretreated with 5,000 units/ml catalase, 2.5 mM aspirin, or 20 mM NAC for 0.5 h, and then Cr(VI) was added. After 3 h of treatment, the cells were subjected to histone protein assay in 24 h. The mean values ± S.D. were from three independent experiments. * indicates a significant increase from control ($p < 0.05$). − indicates a significant decrease from Cr(VI)-treated cells.

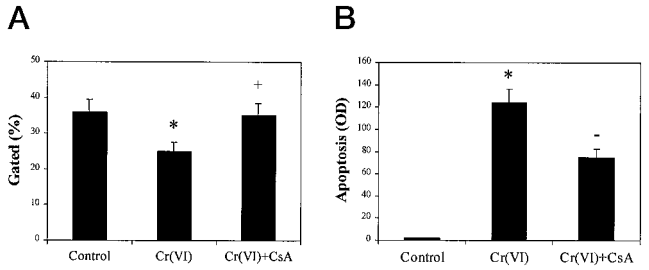

FIG. 9. **Effect of CsA on Cr(VI)-induced apoptosis.** *A*, mitochondrial trans-membrane potential was monitored with JC-1 immediately after 300 μM Cr(VI) treatment for 2 h. The cells were pretreated with 1 μM CsA before Cr(VI) was added. *B*, histone protein assay after CsA treatment. The histone protein assay was carried out at 2 h after a 3-h treatment of the A549 cells with 300 μM Cr(VI). The mean values ± S.D. were from three independent experiments. * indicates a significant increase from control ($p < 0.05$). − indicates a significant decrease from Cr(VI)-treated cells ($p < 0.05$).

erates ROS; (*b*) NADPH and glutathione reductase enhances the ROS generation and Cr(VI)-induced apoptosis; (*c*) Cr(VI)-induced apotosis can be inhibited by antioxidants including catalase, aspirin, and NAC; and (*d*) The apoptotic potential of chromium with different oxidative states is associated with the ability to generate ROS. Among these species, Cr(VI) is most potent in ROS generation and apoptosis induction.

It has been reported that ROS are downstream mediators in the p53-dependent apoptotic pathway (4, 5). The present study demonstrates that Cr(VI) is able to induce activation of p53 protein. p53 protein is a tumor suppressor protein that transmits signals arising from various forms of cellular stress, including DNA damage and hypoxia, to genes and factors that induce cell cycle arrest and apoptosis (31). The p53 signaling pathway can be divided into two parts, upstream of p53 and downstream of p53. The immediate downstream components of the p53 pathway are p53 transactivation targets. The present study shows that an accumulation of p53 protein was induced by Cr(VI) and that p53 is involved in the Cr(VI)-induced apoptosis. It has been reported that a dozen genes can be induced by more than 10-fold when p53 level was increased in the cells. It may be noted that more than half of those genes are directly or indirectly involved in metabolism of ROS, and ROS are required in the p53-dependent apoptotic pathway (4). Because the results obtained from the present study show that antioxidants and enhancers of ROS generation modulate Cr(VI)-induced apoptosis, it appears that ROS generated by p53 activation may also contribute to Cr(VI)-induced apoptosis.

In addition to the p53-dependent pathway, this study also demonstrates that Cr(VI) is able to induce apoptosis through p53-independent pathway. As discussed above, ROS can be generated by two different mechanisms. One is the direct ROS generation in the Cr(VI) reduction process. The other is p53-mediated ROS production. The following observations support the hypothesis that Cr(VI) can induce apoptosis through a p53-independent pathway: (*a*) Cr(VI)-induced mitochondrial damage occurred within 3 h. In this period p53 has not been activated. Blockage of ROS by antioxidants prevented the mitochondrial damage and apoptosis. (*b*) Cr(VI)-induced DNA fragmentation became detectable at the same time when p53 was activated. If the DNA fragmentation was dependent on p53 activation, it should happen after p53 activation. (*c*) Cr(VI) is able to induce apoptosis in the p53-negative cells. At the early stage of apoptotic response, the p53-negative cells and p53-positive cells expressed similar levels of Cr(VI)-induced apoptosis. At the late stage, the p53 wild type cells exhibited a higher level of apoptosis. This indicates that at this stage, Cr(VI) induces apoptosis through both p53-dependent and p53-independent pathways. (*d*) ROS generated by cellular reduction of Cr(VI) occurs within 30 min. In contrast, p53-mediated ROS production can only occur after p53 is activated. This activation process takes a much longer time.

The results obtained from the present study support the following conclusions: (*a*) In the apoptotic signaling pathway, ROS generated from both Cr(VI) reduction and p53 activation play important roles. (*b*) The Cr(VI)-derived ROS initiate apoptosis before activation of p53 protein. (*c*) Although p53 is not required for initiation of Cr(VI)-induced apoptosis, it may enhance apoptosis by transcriptional activation of redox-related

genes. (*d*) Cr(VI) induces apoptosis through both p53-dependent and p53-independent pathways. (*e*) ROS generated by Cr(VI) may play a dual role in the mechanism of Cr(VI)-induced carcinogenesis: genetic damage and apoptosis. The Cr(VI)-induced carcinogenesis may depend on the balance of these two opposite processes. (*f*) it may be speculated that other metal carcinogenes, such as vanadium, cobalt, and nickal, which are also direct ROS-promoting agents (32, 33), may cause apoptosis by a mechanism similar to that of Cr(VI).

REFERENCES

1. Green, D. R., and Reed, J. C. (1998) *Science* **281,** 1309–1312
2. Jabs, T. (1999) *Biochem. Pharmacol.* **57,** 231–245
3. Lotem, J., and Sachs, L. (1996) *Proc. Natl. Acad. Sci. U. S. A.* **93,** 12507–12512
4. Polyak, K., Xia, Y., Zweier, J. L., Kinzler, K. W., and Vogelstein, B. (1997) *Nature* **389,** 300–305
5. Johnson, T. M., Yu, Z. X., Ferrans, V. J., Lowenstein, R. A., and Finkel, T. (1996) *Proc. Natl. Acad. Sci. U. S. A.* **93,** 11848–11852
6. De Flora, S., Bagnasco, M., Serra, D., and Zanacchi, P. (1990) *Mutat. Res.* **238,** 99–172
7. Shi, X., Chiu, A., Chen, C. T., Halliwell, B., Castranova, V., and Vallyathan, V. (1999) *J. Toxicol. Environ. Health B Crit. Rev.* **2,** 87–104
8. Shi, X. L., and Dalal, N. S. (1989) *Biochem. Biophys. Res. Commun.* **163,** 627–634
9. Shi, X. G., and Dalal, N. S. (1990) *Arch. Biochem. Biophys.* **277,** 342–350
10. Shi, X., Mao, Y., Knapton, A. D., Ding, M., Rojanasakul, Y., Gannett, P. M., Dalal, N., and Liu, K. (1994) *Carcinogenesis* **15,** 2475–2478
11. Ye, J., Zhang, X., Young, H. A., Mao, Y., and Shi, X. (1995) *Carcinogenesis* **16,** 2401–2405
12. Shackelford, R. E., Kaufmann, W. K., and Paules, R. S. (1999) *Environ. Health Perspect.* **107,** (Suppl. 1) 5–24
13. Liu, K. J., Shi, X., and Dalal, N. S. (1997) *Biochem. Biophys. Res. Commun.* **235,** 54–58
14. Cossarizza, A., Kalashnikova, G., Grassilli, E., Chiappelli, F., Salvioli, S., Capri, M., Barbieri, D., Troiano, L., Monti, D., and Franceschi, C. (1994) *Exp. Cell Res.* **214,** 323–330
15. Smiley, S. T., Reers, M., Mottola-Hartshorn, C., Lin, M., Chen, A., Smith, T. W., Steele, G. D., Jr., and Chen, L. B. (1991) *Proc. Natl. Acad. Sci. U. S. A.* **88,** 3671–3675
16. Zamzami, N., Marchetti, P., Castedo, M., Decaudin, D., Macho, A., Hirsch, T., Susin, S. A., Petit, P. X., Mignotte, B., and Kroemer, G. (1995) *J. Exp. Med.* **182,** 367–377
17. Zamzami, N., Marchetti, P., Castedo, M., Zanin, C., Vayssiere, J. L., Petit, P. X., and Kroemer, G. (1995) *J. Exp. Med.* **181,** 1661–1672
18. Zamzami, N., Susin, S. A., Marchetti, P., Hirsch, T., Gomez-Monterrey, I., Castedo, M., and Kroemer, G. (1996) *J. Exp. Med.* **183,** 1533–1544
19. Marchetti, P., Castedo, M., Susin, S. A., Zamzami, N., Hirsch, T., Macho, A., Haeffner, A., Hirsch, F., Geuskens, M., and Kroemer, G. (1996) *J. Exp. Med.* **184,** 1155–1160
20. Carter, W. O., Narayanan, P. K., and Robinson, J. P. (1994) *J. Leukocyte Biol.* **55,** 253–258
21. Hockenbery, D. M., Oltvai, Z. N., Yin, X. M., Milliman, C. L., and Korsmeyer, S. J. (1993) *Cell* **75,** 241–251
22. Ye, J., Cippitelli, M., Dorman, L., Ortaldo, J. R., and Young, H. A. (1996) *Mol. Cell. Biol.* **16,** 4744–4753
23. Kroemer, G., Zamzami, N., and Susin, S. A. (1997) *Immunol. Today* **18,** 44–51
24. Bunz, F., Dutriaux, A., Lengauer, C., Waldman, T., Zhou, S., Brown, J. P., Sedivy, J. M., Kinzler, K. W., and Vogelstein, B. (1998) *Science* **282,** 1497–1501
25. Brown, J. M., and Wouters, B. G. (1999) *Cancer Res.* **59,** 1391–1399
26. Lin, D. L., and Chang, C. (1996) *J. Biol. Chem.* **271,** 14649–14652
27. Rubin, S. J., Hallahan, D. E., Ashman, C. R., Brachman, D. G., Beckett, M. A., Virudachalam, S., Yandell, D. W., and Weichselbaum, R. R. (1991) *J. Surg. Oncol.* **46,** 31–36
28. Snyder, R. D. (1988) *Mutat. Res.* **193,** 237–246
29. Chen, F., Ye, J., Zhang, X., Rojanasakul, Y., and Shi, X. (1997) *Arch. Biochem. Biophys.* **338,** 165–172
30. Kataoka, M., Tonooka, K., Ando, T., Imai, K., and Aimoto, T. (1997) *Free Radical Res.* **27,** 419–427
31. Prives, C. (1998) *Cell* **95,** 5–8
32. Leonard, S., Gannett, P. M., Rojanasakul, Y., Schwegler-Berry, D., Castranova, V., Vallyathan, V., and Shi, X. (1998) *J. Inorg. Biochem.* **70,** 239–244
33. Shi, X., Dalal, N. S., and Kasprzak, K. S. (1992) *Arch. Biochem. Biophys.* **299,** 154–162